Multistep Magnetization Plateaus in the Shastry-Sutherland System TbB_4

S. Yoshii,[1,*] T. Yamamoto,[1] M. Hagiwara,[1] S. Michimura,[2] A. Shigekawa,[2] F. Iga,[2] T. Takabatake,[2] and K. Kindo[3]
[1]KYOKUGEN, Osaka University, 1-3 Machikaneyama, Toyonaka, Osaka 560-8531, Japan
[2]ADSM, Hiroshima University, Higashi-Hiroshima 739-8530, Japan
[3]Institute for Solid State Physics, University of Tokyo, Kashiwa 277-8581, Japan
(Received 4 September 2007; revised manuscript received 18 June 2008; published 20 August 2008)

We report high-field magnetization and magnetostriction measurements on the rare-earth-metal tetraboride TbB_4, in which the Tb moments form a Shastry-Sutherland lattice in the tetragonal basal plane. A number of magnetization plateaus appear when the magnetic field is perpendicular to the magnetic easy plane. We propose that the magnetization plateaus arise from the combined effect of magnetic frustration and quadrupole interaction in the unique two-dimensional network.

DOI: 10.1103/PhysRevLett.101.087202 PACS numbers: 75.10.Hk, 75.30.Gw

Magnetic properties of systems with geometrical frustration have been one of the hot issues in condensed-matter physics during the last three decades. The triangular or the pyrochlore lattice compounds have been extensively investigated because of unusual phenomena, such as an unconventional spin freezing state in the triangular lattice antiferromagnet $NiGa_2S_4$ [1,2] or a spin-driven Jahn-Teller effect discussed for some chromium spinel compounds [3]. Furthermore, some ferromagnetic pyrochlore compounds with uniaxial anisotropy show a novel spin-ice state as found in $Dy_2Ti_2O_7$ [4].

Recently, rare-earth-metal tetraborides RB_4 have intensively been investigated, in which geometrical frustration originates from a unique two-dimensional (2D) lattice network. It crystallizes in the tetragonal structure ($P4/mbm$) and the network of magnetic R ions in the (001) plane is characterized by orthogonal dimers that is equivalent to the Shastry-Sutherland lattice (SSL) [5] [see the inset of Fig. 1(a)]. Magnetic frustration exists when the near-neighbor interactions J_1 and J_2 are antiferromagnetic. Strong magnetic frustration leads to interesting phenomena such as magnetization plateaus found in one of the SSL compounds $SrCu_2(BO_3)_2$ [6]. The plateaus are interpreted as the solidification of hopping triplets due to the effective repulsive interaction and limited hopping caused by strong frustration [7].

In contrast to the quantum spin system $SrCu_2(BO_3)_2$, RB_4 has a classical spin. RB_4 compounds with $R =$ Tb, Dy, Ho, Er, and Tm exhibit successive magnetic phase transitions [8], which evidences the existence of competing interactions. An effect of magnetic frustration in RB_4 manifests itself as a magnetization plateau at a half of the saturation magnetization as observed in the Ising-spin system ErB_4 [9] or TmB_4 [10]. It was pointed out that the competition of the Zeeman effect and frustration due to J_1 and J_2 must be an origin of the plateau. Recent studies also revealed an importance of the geometrical quadrupolar frustration, as discussed for DyB_4 [11].

In this Letter, we report the studies on the multiple phase transitions in TbB_4 by means of high-field magnetization and magnetostriction measurements up to 54 T. We remarkably found that a number of magnetization plateaus appear when the magnetic field is perpendicular to the magnetic easy plane. Usually, metamagnetic transitions in rare-earth-metal compounds with Ising anisotropy are expected when a magnetic field is applied along the easy axis. Thus it is very interesting to understand the origin of multistep magnetization in TbB_4 from the elucidation of the mechanism of phase transitions in the frustrated antiferromagnet. We have also found symmetric field positions of the magnetization jumps with respect to the center field of the $1/2$ magnetization plateau. As will be described later, the analysis of magnetization indicates a significant role of magnetic frustration and quadrupole interaction in the magnetic properties of the unique two-dimensional lattice system TbB_4.

Single crystals of TbB_4 were grown by a floating-zone method. The magnetization was measured by an induction method. The magnetostriction was measured by using a strain gauge. The high-field measurements up to 54 T were performed by using a pulse magnet.

TbB_4 shows successive antiferromagnetic transitions at $T_{N1} = 44$ K and $T_{N2} = 24$ K [8]. Magnetic moments below T_{N1} lie in the c plane and have a noncollinear configuration [12]. The magnetic unit consists of four spins in the crystal unit cell. The magnetic moments point toward the equivalent [110] direction between T_{N1} and T_{N2}. Below T_{N2}, moments slightly tilt from the diagonal direction. A quadrupole interaction is suggested as an origin of this tilt, since there is no difference in energy between these two structures in the Heisenberg-type bilinear interaction and the simple local anisotropy prefers the magnetic structure between T_{N1} and T_{N2}.

Figure 1(a) shows the high-field magnetization M at 4.2 K. The magnetization process for the magnetic easy (001) plane is characterized by one large jump at $B_c = 16$ T for $B \parallel [100]$ and at $B_c = 12$ T for $B \parallel [110]$. The different transition fields and different heights of the magnetization jumps along the [100] and the [110] directions suggest a magnetic anisotropy within the (001) plane.

 © 2008 The American Physical Society

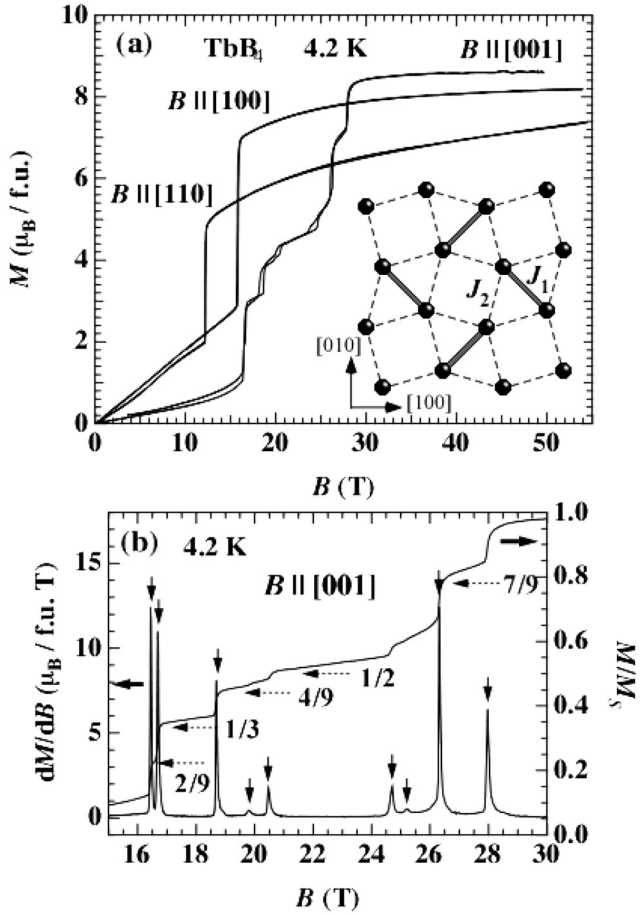

FIG. 1. (a) Magnetization (M) of TbB_4 at 4.2 K for magnetic fields B applied along the [100], [110], and [001] axes. Inset: network of Tb atoms in the (001) plane. The solid and dashed lines denote the nearest- and the next-nearest-neighbor exchange interactions, respectively. (b) Comparison of the field derivative magnetization dM/dB along the [001] axis with M. The indicated fractions denote the ratio M/M_s.

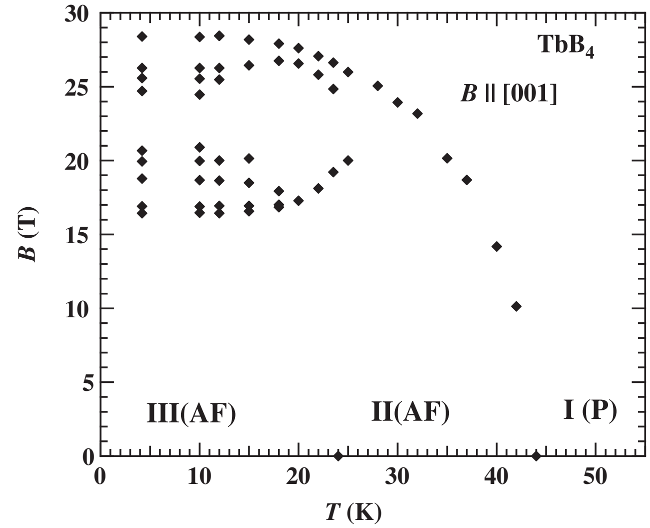

FIG. 2. Magnetic phase diagram of TbB_4 for $B \parallel [001]$.

The most remarkable observation is the appearance of successive metamagnetic transitions along the hard [001] direction. The field derivative of magnetization dM/dB in Fig. 1(b) displays at least nine transitions above 16 T up to the saturation field $B_s = 28$ T. The magnetization exhibits plateaus at 2/9, 1/3, 4/9, 1/2 and other fractions of the saturation magnetization M_s of $8.6\mu_B/$[formula units (f.u.)], which is close to the free Tb^{3+} moment of $9\mu_B$ where μ_B is the Bohr magneton. A close look at dM/dB demonstrates that the interval of the transition field and the height of magnetization jump appear symmetrically to the field around 22.3 T where the $1/2M_s$ state exists.

Figure 2 shows the magnetic phase diagram for $B \parallel [001]$ obtained from the magnetization measurements. The multistep magnetization disappears above T_{N2} (24 K). The saturation field B_s, which corresponds to the peak of dM/dB at the highest field, goes to zero when approaching T_{N1} (44 K).

As is well known, steplike magnetization has been found in many rare-earth-metal intermetallics with Ising-type anisotropy. The famous one is CeSb [13], which is regarded as a one-dimensional Ising chain and is an example of the devil's staircase. In such systems, the steplike magnetization has been explained by flips of spins. In TbB_4, the multistep magnetization appears along the hard axis and is quite different from that in the Ising system. It is usually expected that a magnetic field perpendicular to the easy axis or plane causes rotation of the moments toward the field direction, eventually leading to a forced-ferromagnetic arrangement of the moments.

In TbB_4, the easy-plane anisotropy is ascribed to the crystalline electric field (CEF) effect acting on the $4f$ multiplet of Tb^{3+} ($J = 6$). The CEF Hamiltonian of the tetragonal system is given by $H_{\mathrm{CEF}} = B_2^0 O_2^0 + B_4^0 O_4^0 + B_4^4 O_4^4 + B_6^0 O_6^0 + B_6^4 O_6^4$, where the B_l^m are the CEF parameters and the O_l^m are the Stevens equivalent operators. The B_2^0 value is estimated from the magnetic susceptibilities χ under a mean-field treatment by using the relations

$$B_2^0 = 10(\theta_p^{[100]} - \theta_p^{[001]})/3(2J-1)(2J+3),$$
$$\chi^i = C/(T + \theta_p^i) = \chi_{\mathrm{CEF}}^i/(1 - \lambda\chi_{\mathrm{CEF}}^i), \quad (i = [100], [001]), \tag{1}$$

where $\theta_p^{[100]}$ and $\theta_p^{[001]}$ are the paramagnetic Curie temperatures derived from the magnetic susceptibilities along the [100] and [001] directions, respectively, J is the total angular momentum of the Tb^{3+} ion, C is the Curie constant, χ_{CEF} is a magnetic susceptibility due to the CEF alone, and λ is a mean-field parameter.

From Eq. (1), the values B_2^0/k_B and λ are evaluated to be 0.6 K and -3.3 mol/emu, respectively. The calculated χ reproduces the experimental results rather well in the paramagnetic region, as shown in Fig. 3, and the magnetic anisotropy is ascribed to the CEF effect.

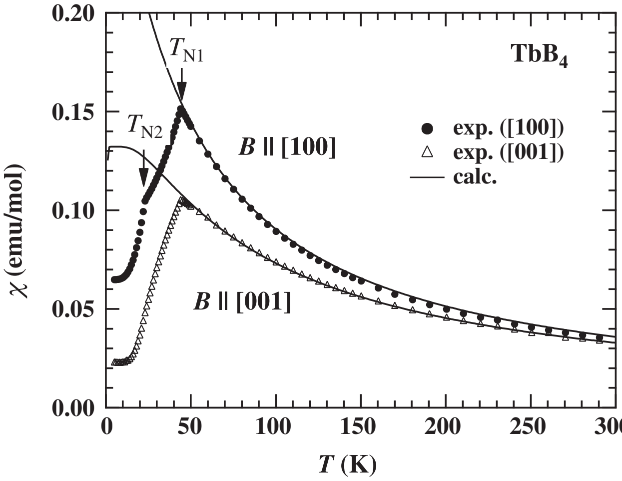

FIG. 3. Magnetic susceptibility of TbB_4 for $B \parallel [100]$ and $B \parallel [001]$. The solid lines indicate the calculated paramagnetic susceptibility for $B_2^0/k_B = 0.6$ K and $\lambda = -3.3$ emu/mol.

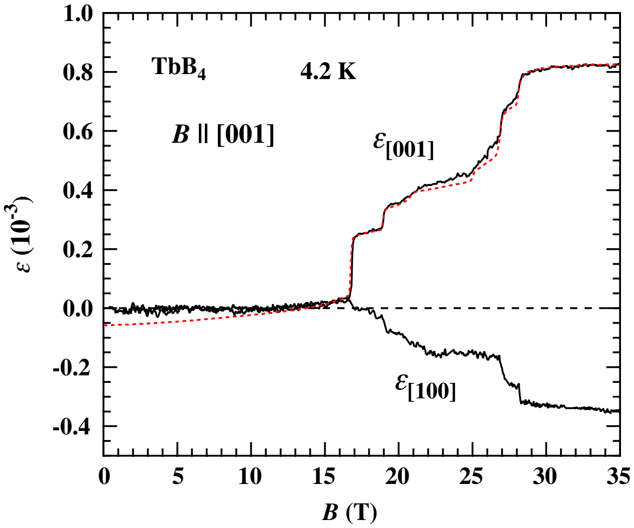

FIG. 4 (color online). Longitudinal magnetostriction $\epsilon_{[001]}$ ($\Delta L/L \parallel [001]$) and transverse magnetostriction $\epsilon_{[100]}$ ($\Delta L/L \parallel [100]$) of TbB_4 at 4.2 K for $B \parallel [001]$. The relative change of the magnetization ($B \parallel [001]$, dotted line) is compared with $\epsilon_{[001]}$.

In the magnetically ordered region, the small initial slope below 10 T in the magnetization M curve along the [001] axis, compared with that in the basal plane, can result from a small $\langle J_z \rangle$ value of the CEF ground state such as $|0\rangle$ and $|\pm 1\rangle$. The analysis of χ suggests a total splitting of the CEF states of about 100 K. To convince the reader that the metamagnetic behavior along the [001] axis cannot be simply explained by a successive level crossing between the ground state and various excited CEF states with larger $\langle J_z \rangle$ at low temperatures, we examined a low temperature magnetization for various sets of CEF parameters. However, the nine steps and the unique interval of the transitions and the height of magnetization jumps ΔM are not obtained.

Magnetostriction also denies the single site CEF effect as a predominant source of the metamagnetic transitions. Figure 4 shows the magnetostriction $\epsilon = \Delta L/L$ at 4.2 K for $B \parallel [001]$. The observed stepwise behavior is very similar to the magnetization curve along the [001] axis, and excellent agreement is found between the magnetization and $\epsilon_{[001]}$ after being normalized by the saturation value. The crystal expands along the [001] direction, while it shrinks along the [100] direction. Based on the CEF analysis, using the Stevens equivalent operators, the strain along the z axis with the same field direction is described by $\epsilon_{zz} \propto \langle O_2^0 \rangle$, where $O_2^0 = 3J_z^2 - J(J+1)$ [14]. Then, a stepwise increase of $\langle J_z \rangle$ produces a jump of the strain ϵ_{zz}. However, the excellent proportionality $\epsilon_{zz} \propto M$ observed in the experiment does not agree with the relation $\epsilon_{zz} \propto M^2$. Thus the metamagnetic behavior along the [001] axis must be a cooperative phenomenon.

The importance of the 2D model with antiferromagnetic J_1 and J_2 interactions as shown in Fig. 1(a) was recognized as the appearance of the magnetization plateau in the Ising system ErB_4 [9]. The importance of this model was also recognized in GdB_4. According to the original study by Shastry and Sutherland [5], the ground state in the classical Heisenberg system has helical long-range order for $J_1/J_2 > 1$. The ratio $J_1/J_2 = 13$ derived from the magnetization study in GdB_4 [15] is in accordance with the non-collinear magnetic structure [16].

In order to examine the 2D model for TbB_4, we calculate M along the [100] and [110] directions by the mean-field approximation and compare them with the experimental curves. Based on the magnetic structure as determined in a neutron-diffraction study [12], we consider four magnetic sublattices which consist of two orthogonal dimers in the (001) plane (see Fig. 5), and ferromagnetic alignment of moments along the [001] direction. In this case, the free energy is given by $E = E_{\rm exch} + E_{\rm bq} + E_{\rm aniso} + E_{\rm Zeeman}$. The $E_{\rm exch}$ represents the bilinear exchange interaction $-J_i \vec{S}_j \cdot \vec{S}_k$. The $E_{\rm bq}$ corresponds to a biquadratic interaction $-b_i(\vec{S}_j \cdot \vec{S}_k)^2$, which is related to the magnetoelastic effect [17]. For J_i and b_i, we take the interaction constants between the nearest-neighbor (J_1, b_1) and the next-nearest-neighbor (J_2, b_2) pairs. For $B \parallel [100]$ and $B \parallel [110]$, the magnetic moments are assumed to be confined to the (001) plane due to a dominant easy-plane anisotropy. The in-plane anisotropy is taken into account because the Tb site has a local two-fold axis directed to one of the equivalent [110] axes. The $E_{\rm aniso}$ represents the in-plane anisotropy energy of $S^2 \sum_i K \sin^2\theta_i$ ($i = 1, 2, 3, 4$), where θ_i is the angle from the local two-fold axis at the site i. The $E_{\rm Zeeman}$ is a Zeeman term, in which a Landé factor $g = 3/2$ and a composite spin $S = 6$ are assumed for Tb^{3+} ions.

Using $J_1/k_B = -1.55$ K, $J_2/k_B = -0.33$ K, $b_1/k_B = -0.025$ K, $b_2/k_B = 0.0012$ K, and $K/k_B = 2.5$ K, the initial slope of M, the transition field, and the height of the magnetization jump are satisfactorily reproduced for both $B \parallel [100]$ and $B \parallel [110]$ (Fig. 5). Thus, the 2D model

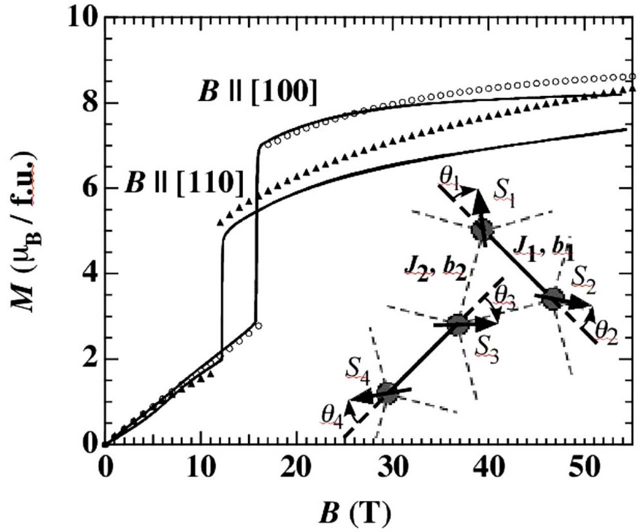

FIG. 5 (color online). Calculated M for $B \parallel [100]$ (circles) and $B \parallel [110]$ (triangles). The solid lines are experimental curves. The calculation parameters are $J_1/k_B = -1.55$ K, $J_2/k_B = -0.33$ K, $b_1/k_B = -0.025$ K, $b_2/k_B = 0.0012$ K, and $K/k_B = 2.5$ K. Inset: Schematic of the configuration of four sublattice moments. The solid and dashed lines denote the nearest-neighbor and the next-nearest-neighbor interactions, respectively.

can be applied and TbB_4 can be regarded as a SSL system with easy-plane anisotropy. We emphasize that the biquadratic contribution to the total energy is comparable to that of the exchange interaction, and that the biquadratic term is intrinsically needed to explain the strong suppression of M at high fields and to explain that the saturation field in the (001) plane is higher than along the [001] direction. Because of the large magnetostriction in TbB_4, as shown in Fig. 4, the biquadratic term is ascribed to the magnetoelastic effect, which may be attributed to the quadrupole interaction [18], as commonly discussed for $4f$-electron systems [19]. Interestingly, the nearest-neighbor biquadratic constant b_1 has negative sign, which prefers an orthogonal configuration of the nearest-neighbor magnetic moments. This is consistent with the bending of M above the transition field.

The magnetization plateaus in the antiferromagnet TbB_4 along the [001] direction must originate from a cooperative reorientation of the Tb moments. One plausible scenario is a combined effect of a quadrupole interaction and the competing magnetic interactions. Usually in $4f$ systems, the magnetic moment strongly couples to the quadrupole moment. Then, by applying a magnetic field along the [001] axis, the rotation of the magnetic moment is accompanied by the rotation of the quadrupole axis. Because the quadrupole moment has an anisotropic charge distribution, such rotation of the quadrupole moment costs the Coulomb energy. To gain this energy, the lattice expands along the c axis and shrinks in the c plane, thus explaining the observed sign of the magnetostriction. If an antiferroquadrupolar interaction acts between the quadrupole moments, it prefers an orthogonal configuration of the quadrupole axis, or of magnetic moment, from one site to the other. Then, owing to a complex interplay between the frustrated bilinear interaction, quadrupole interaction, and Zeeman interaction, a reorientation of magnetic moments may occur step by step with increasing magnetic field. To understand the interaction mechanism in TbB_4 completely, experimental investigations of magnetic structures by microscopic techniques in high magnetic fields are highly desired.

In summary, the magnetization plateaus in TbB_4 appear only along the magnetic hard direction of the [001] axis. This is quite different from the traditional Shastry-Sutherland compound $SrCu_2(BO_3)_2$, in which a number of plateaus appear for both $B \parallel [001]$ and $B \perp [001]$ [20]. We pointed out the importance of the biquadratic interaction in the magnetization process in TbB_4 and propose that the magnetization plateaus must arise from not only the frustrated J_1 and J_2 interactions in the SSL model but also the biquadratic interactions probably originating from the quadrupole interaction.

This work was supported by the 21st Century COE Program named "Towards a new basic science: depth and synthesis," and by a Grant-in-Aid for Scientific Research on Priority Areas "High-Field Spin Science in 100 T" (No. 451) and Fundamental Research C (No. 16540319) from the Ministry of Education, Culture, Sports, Science, and Technology of Japan.

*yoshii@imr.tohoku.ac.jp

[1] S. Nakatsuji *et al.*, Science **309**, 1697 (2005).
[2] H. Takeya *et al.*, Phys. Rev. B **77**, 054429 (2008).
[3] H. Ueda *et al.*, Phys. Rev. Lett. **94**, 047202 (2005).
[4] M. J. Harris *et al.*, Phys. Rev. Lett. **79**, 2554 (1997).
[5] B. S. Shastry and B. Sutherland, Physica (Amsterdam) **108B+C**, 1069 (1981).
[6] H. Kageyama *et al.*, Phys. Rev. Lett. **82**, 3168 (1999).
[7] See, for example, S. Miyahara and K. Ueda, J. Phys. Condens. Matter **15**, R327 (2003).
[8] Z. Fisk *et al.*, Solid State Commun. **39**, 1189 (1981).
[9] S. Michimura *et al.*, Physica (Amsterdam) **378B–380B**, 596 (2006).
[10] F. Iga *et al.*, J. Magn. Magn. Mater. **310**, E443 (2007).
[11] R. Watanuki *et al.*, J. Phys. Soc. Jpn. **74**, 2169 (2005).
[12] T. Matsumura *et al.*, J. Phys. Soc. Jpn. **76**, 015001 (2007).
[13] J. Rossat-Mignot *et al.*, J. Magn. Magn. Mater. **31–34**, 398 (1983).
[14] P. Morin *et al.*, Phys. Rev. B **37**, 5401 (1988).
[15] A. Kikkawa *et al.*, J. Phys. Soc. Jpn. **76**, 024711 (2007).
[16] J. A. Blanco *et al.*, Phys. Rev. B **73**, 212411 (2006).
[17] K. Penc *et al.*, Phys. Rev. Lett. **93**, 197203 (2004).
[18] J. Sivardiere, J. Magn. Magn. Mater. **1**, 23 (1975).
[19] P. Morin and D. Schmitt, *Ferromagnetic Materials*, edited by K. H. J. Bushow and E. P. Wohlfarth (Elsevier, Amsterdam, 1990) Vol. 5, p. 1.
[20] K. Onizuka *et al.*, J. Phys. Soc. Jpn. **69**, 1016 (2000).